Talanta 210 (2020) 120648

Contents lists available at ScienceDirect

Talanta

journal homepage: www.elsevier.com/locate/talanta

Genosensors for differential detection of Zika virus

Daniel Alzate[a], Sebastian Cajigas[a], Sara Robledo[b], Carlos Muskus[b], Jahir Orozco[a,*]

[a] Max Planck Tandem Group in Nanobioengineering, University of Antioquia, Complejo Ruta N, Calle 67 N° 52–20, Medellín, 050010, Colombia
[b] Programa de Estudio y Control de Enfermedades Tropicales (PECET), Facultad de Medicina, Universidad de Antioquia, Calle 62 N° 52-59, Medellín, Colombia

ARTICLE INFO

Keywords:
Genosensors
Zika-virus
Differencial-detection
Electrochemistry
Bioinformatics

ABSTRACT

Zika virus (ZIKV) is considered an emerging infectious disease of high clinical and epidemiological relevance. The epidemiological emergency generated by the virus in Latin America and Southeast Asia in 2014 evidenced the urgent need for rapid and acute diagnostic tools. The current laboratory diagnosis of ZIKV is based on molecular and serological methods. However, molecular tools need expensive and sophisticated equipment and trained personnel; and serological detection may suffer from cross-reactivity. In this context, genosensors offer an attractive alternative for field-ready, early and accurate diagnosis of ZIKV. This work reports on the development of genosensors for the differential detection of ZIKV and its discrimination from dengue (DENV) and chikungunya (CHIKV) homologous arboviruses. We designed specific capture and signal probes by bioinformatics, and prove their specificity to amplify the target genetic material by the polymerase chain reaction (PCR). The designed biotinylated capture and digoxigenin (Dig)-labeled signal probes hybridized the target in a sandwich-type format. An anti-Dig antibody labeled with the horseradish peroxidase (HRP) enzyme allowed for both optical and electrochemical detection. The genosensors detected the ZIKV genetic material in spiked serum, urine, and saliva samples and cDNA from infected patients, discriminating them from the DENV and ZIKV genetic material. The proposed system offers a step forward to the differential diagnosis of the ZIKV, closer to the patient, very promising for diagnosis and surveillance of this rapidly emerging disease.

1. Introduction

ZIKV has become a global health care challenge since the infection has spread from tropical regions to other areas. People have been infected with the ZIKV in more than 50 countries around the world, since the beginning of 2015, when the more recent Zika virus outbreak occurred [1]. The virus is mostly transmitted by mosquitos of the *Aedes* genus, which are ubiquitous in many tropical areas but with global climate change they are migrating to non-tropical regions. Frequent symptoms of the infection include fever, rash, headache and joint pain, conjunctivitis and muscle pain, which are difficult to distinguish clinically from DENV and CHIKV infections [2]. Therefore, accurate and early diagnosis is crucial, especially for pregnant women who if infected with the ZIKV in the first trimester of pregnancy have an elevated risk of delivering a newborn with microcephaly or acute neurological syndromes [3,4]. The ZIKV has been also associated with the development of Guillain-Barré syndrome and ophthalmological disorders [5].

The current laboratory diagnosis of ZIKV is based on the detection of the viral material by reverse transcriptase real-time polymerase chain reaction (RT real-time PCR) RNA and serological detection of anti-ZIKV antibodies [6]. The molecular method is the gold standard for the detection of viral RNA, but it has high requirements for equipment and trained personnel. In the serologic method, antibodies may cross-react with other flaviviruses, such as DENV and CHIKV, which are prevalent in the same endemic regions. A viral culture is an alternative to confirming the infection, but this is highly time-consuming. Therefore, there is an urgent need for new, rapid, simple, and sensitive ZIKV diagnostic tests. In this context, features of genosensors, in terms of specificity, sensitivity, and speed of response, offer remarkable opportunities for differential diagnosis of the ZIKV. Currently, there are only a few electrochemical genosensors reported in the literature for ZIKV detection. For example, a pencil carbon graphite electrode modified with a 3-amino-4-hydroxybenzoic acid derivative for the detection of ZIKV DNA by square-wave voltammetry, with a limit of detection (LOD) of 25.4 pmol L^{-1} [7]. An impedimetric genosensor for label-free detection of ZIKV at disposable polyethylene terephthalate-based electrodes covered with a nanometric gold layer, with a LOD of 25 nmol L^{-1} [8]. Some other few authors have reported ZIKV biosensors based on either immune/fluorescence detection [9–11] and detection of ZIKV nanoparticles based on a molecularly printed polymer [12].

* Corresponding author.
E-mail address: grupotandem.nanobioe@udea.edu.co (J. Orozco).

https://doi.org/10.1016/j.talanta.2019.120648
Received 3 October 2019; Received in revised form 12 December 2019; Accepted 13 December 2019
Available online 16 December 2019
0039-9140/

This work reports on the development of genosensors for the differential detection of ZIKV and its discrimination from DENV and CHIKV homologous arboviruses. The methodology involves searching for phylogenetically conserved nucleotide sequences to function as the target, screened from a databank by rigorous bioinformatics analysis. Then, based on the selected targets, we designed specific primers for target amplification and the corresponding capture and signal probes for the genosensor arrangement. The primers and molecular probes were tested by both real-time and conventional PCR. Results demonstrated that the probes amplified not only the synthetic target DNA but also RNA from the virus replicated in cultures and from infected patients, in a very specific manner. The designed biotinylated capture and Dig-labeled signal probes hybridized the target in a sandwich-type format. An anti-Dig antibody labeled with the HRP enzyme allowed for both a bench spectrophotometric detection and electrochemical detection of the ZIKV with a portable potentiostat. Although biosensors have been developed for the detection of multiple pathogens [13–17], this is the first DNA strand-based electrochemical genosensor for differential detection of ZIKV, studied in conditions closer to a real scenario. The genosensor discriminated the ZIKV from the DENV and ZIKV genetic material in spiked serum, urine, and saliva samples; and cDNA and RNA from infected patients. The proposed system paves the way towards the development of a sensitive and specific test for the differential diagnosis of the ZIKV, closer to the patient, at the point of care.

2. Materials and methods

The reagents and solutions, screen-printed gold electrodes (SPAuEs) and equipment, characterization of the transducer platform, RNA extraction and amplification methods are described in the supporting information (S.I) section. Activation of the electrodes and testing of their electrochemical performance was achieved based on protocols reported elsewhere [18]. Bioinformatics design, optimization of the genosensor development and of the genetic material in physiological samples are detailed in the S.I. section and summarized herein as follow.

2.1. Bioinformatics design

To design a generic genosensor that allows for the detection of the ZIKV, we downloaded whole-genome sequences from all different viruses reported in the last 7 years, and filter and aligned them to define the conserved regions. After discarding all viral sequences isolated from non-human species, and excluding incomplete sequences, we found ten fully conserved regions from which we finally selected four targets based on thermodynamic and molecular probe design criteria. For each of the four targets, we designed forward and reverse primers for amplification by PCR, and a 3′-end biotinylated capture probe and a 5′ end Dig-labeled signal probe for assembling the genosensor. The selected probes are listed in Table 1.

2.2. Optimization of the genosensor development

The genosensor was optimized by assembling the capture, target and signal probes described in Table S2 onto the surface of neutravidin coated polystyrene microplates, with proper washing and blocking steps in between. The incubation temperature for hybridization was based on findings summarized in Table S2. Anti-Dig-HRP was added to bind to the signal probe and washed 6 times. Subsequently, a TMB solution containing 10 mM H_2O_2 was added to each well while stirring at 800 rpm for 30 min, and the color intensity produced was read on a spectrophotometer at a wavelength of 620 nm for quantification. Once optimized, the genosensor was assembled on streptavidin-coated magnetic particles by following the same steps described above and further attracted to the surface of the SPAuE by a magnet. The electrochemical signal coming from the reduction of TMB was recorded by chronoamperometry after applying a constant voltage of −150 mV for 60 s. The Limit of Detection (LOD) of the genosensors was estimated according to the 3-sigma criterion, where the LOD is three times the standard deviation of the blank divided by the slope of the calibration curve [19].

2.3. Detection of genetic material in physiological samples

To detect the genetic material in physiological samples, we challenged the genosensor R1 with saliva, serum, and urine samples from a 26 years old healthy subject spiked with ZIKV, DENV, and CHIKV synthetic sequences not only at equimolar concentrations but also with a 1000-fold excess of DENV and CHIKV with respect to the ZIKV concentration. We tested the response in samples of cDNA from three patients infected with the virus after reverse RNA transcription, and RNA from an infected patient after denaturation; and contrasted with the respective negative control.

3. Results and discussion

Genosensors are built by the bioreceptor, a DNA strand attached to a solid platform, that interacts specifically with the target strand by complementary Watson and Crick base pairing. The recognition event is converted into an output signal in a signal-concentration dependent manner. Herein, detection of the target nucleic acid is achieved in a sandwich format in between a biotin-labeled capture probe and an adjacent signal probe labeled with Dig [20,21]. The biotinylated capture probe was first anchored to streptavidin-coated magnetic beads (Fig. 1A, **step 1)**. The molecular target pre-hybridizes first with the signal probe (**step 2**) and once in between the capture and signal probes, the hybrid is coupled with an anti-Dig antibody labeled with HRP (**step 3**) to follow the target concentration. The resultant bioconjugate is attracted to the working electrode surface of a screen-printed electrode (SPE, Fig. 1B). The quantification is achieved by the electrochemical signal produced when the TMB enzymatically-oxidized product is reduced back at the SPE surface (Fig. C). Dual or multiple SPEs allow for differential detection as shown later. The enzymatic reaction generates a colored product that can be also followed by spectrophotometry. The intensity of the signal is proportional to the amount of DNA (RNA) hybridized in either of the mentioned biosensor formats [22].

3.1. Bioinformatic design

After downloading sequences from all different virus lineages reported in the NCBI database in the last 7 years, as described in the experimental section, we selected the conserved regions and designed probes for the development of a generic genosensor that allows for detection of the ZIKV from any place worldwide. The rational bioinformatic analyzes allowed the selection of 10 fully conserved target sequences detailed in the Supporting Information (S.I) Table S1, including the sequence, number of nucleotides, and position in the ZIKV genome. From the phylogenetically conserved regions, we selected the only four regions that have an appropriate length to be assembled in the biosensor format and fulfill all the thermodynamic and molecular probe design criteria, as detailed in the materials and methods from the S.I. section. We designed forward and reverse primers for amplification by PCR, and a 3'end biotinylated capture probe and a 5'end Dig-labeled signal probe for assembling the genosensor, per each of the four selected targets. For DENV and CHIKV, the sequences were selected based on the literature [23–27], since they are highly reported primers for the clinical diagnosis of such arbovirosis. The selected DNA probes are listed in Table 1.

Table 1
ZIKV molecular targets, amplification primers and detection probes.

REGION	PHILOGENETICALLY CONSERVED REGIONS (5′-3′)
R1	TCATCTGTGCCAGTTGATTGGGTTCCAACTGGGAGAACTACCTGGTCAATCCATGGAAAGGGAGAATGGATGACCA
R2	ATGGGAAAAAGAGAAAAGAAACAAGGGGAATTTGGAAAGGCCAAGGGCAGCCGCGCCATCTGGTATATGTGGC
R5,1	AAAAGCAACACCATAAAAAGTGTGTCCACCACGAGCCAGCTCCTCTTGGGGCGCATGGACGGGCC
R5,2	AAAAGCAACACCATAAAAAGTGTGTCCACCACGAGCCAGCTCCTCTTGGGGCGCATGGACGGGCC

REGION	PRIMERS	
	FORWARD	REVERSE
R1	5′-ACTGGGAGAACTACCTGGTC-3′	5′-GGTCATCCATTCTCCCTTTCC-3′
R2	5′-CAAGGGGAATTTGGAAAGGC-3′	5′-GCCACATATACCAGATGGCG-3′
R5,1	5′-GTGTCCACCACGAGCCAG-3′	5′-CATGCGCCCCAAGAGGAG-3′
R5,2	5′-TCCACCACGAGCCAGCTC-3′	5′-GTCCATGCGCCCCAAGAG-3′
CHIKV	5′-AAGCTYCGCGTCCTTTACCAAG-3′	5′-CCAAATTGTCCYGGTCTTCCT-3′
DENV	5′-AAGGACTAGAGGTTAGAGGAGACCC-3′	5′-CGTTCTGTGCCTGGAATGATG-3′

REGION	CAPTURE PROBE	SIGNAL PROBE	T/°C
R1	5′-GATTGACCAGGTAGTTCTCCCAGT/3′Bio	5′Dig/GGTCATCCATTCTCCCTTTCCATG-3′	55
R2	5′-CCTTGGCCTTTCCAAATTCCCCTTG/3′Bio	5′Dig/GCCACATATACCAGATGGCGCGGCT-3′	50
R5,1	5′- CTGGCTCGTGGTGGACAC/3′Bio	5′Dig/CATGCGCCCCAAGAGGAG-3′	60
R5,2	5′- GAGCTGGCTCGTGGTGGA/3′Bio	5′Dig/GTCCATGCGCCCCAAGAG-3′	60

3.2. Optimization of the genosensor development

Because we started with a new set of probes that were not reported before in the literature, we first needed to verify the specificity of the target regions and primers designed *in silico* before assembling the genosensor. For this purpose, we tested the amplification of the four selected target regions with their corresponding designed primer pairs by conventional PCR, whose amplification products were detected by agarose gel electrophoresis as shown in S.I Fig. S1A. The results show that the designed molecular primers were specific for the efficient amplification of the synthetic ZIKV target probes as compared with a reference molecular weight ladder and negative control with non-genetic material. Indeed, these primers efficiently amplified also cDNA transcribed from RNA strands from the ZIKV replicated in cell cultures (S.I Fig. S1B). The primers also specifically amplified RNA from samples of infected cell cultures and discriminated them from the DENV and CHIKV genetic material by real-time PCR (S.I Fig. S1C). These results demonstrated that the high specificity of the designed primers allows us to detect RNA from the ZIKV and discriminate it from the phylogenetically related arbovirus DENV and CHIKV. Rigor employed in the bioinformatic design ensures reliability on a potential diagnosis of a patient infected with these viruses and reduces the probability of recovering false positives.

The next set of experiments optimized all the variables involved in the genosensor assembly. The process was readily achieved by spectrophotometry in a microplate format by taking advantage of the colored product generated by the enzymatic oxidation of TMB. Concentrations of neutravidin, capture and signal probes and anti-Dig-HRP, as well as the hybridization temperature and the incubation time necessary to maximize the colorimetric response, with a fixed concentration of 50 nmol L^{-1} molecular target were optimized. 0.1 to 10 μgmL^{-1} neutravidin was tested to attach to the polystyrene ELISA-like dishes by physical absorption. The colorimetric signal reaches a plateau after 3 μgmL^{-1} of neutravidin, indicating the wells saturation point.

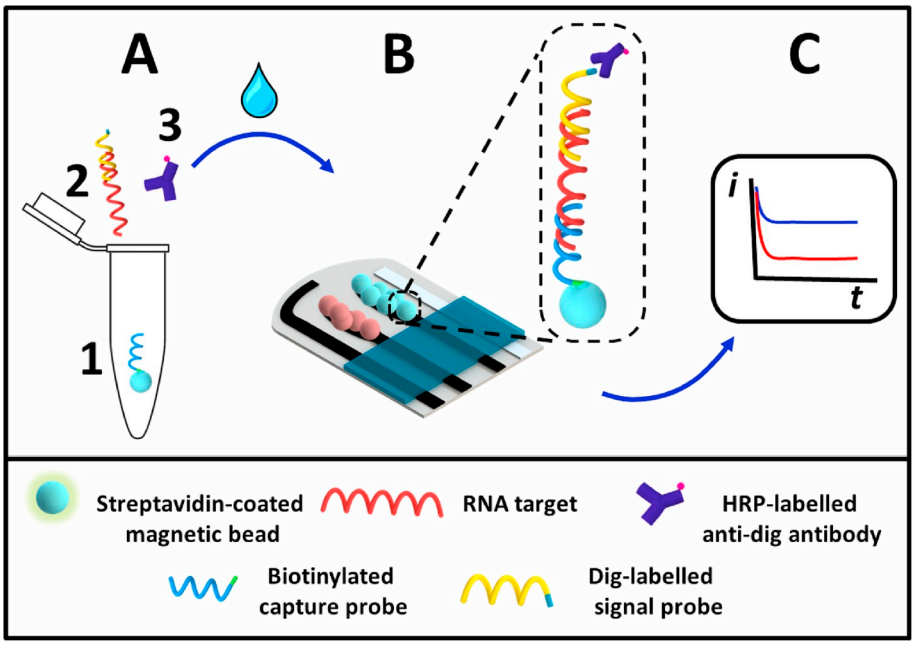

Fig. 1. Scheme of an electrochemical genosensor. A) Genosensor assembly steps. **1. A)** specific biotinylated capture probe is immobilized at streptavidin-coated magnetic beads. **2.** The target is pre-hybridized with the Dig-labeled signal probe and further added to the capture probe-coated magnetic beads to hybridize. **3.** Recognition of the signal probe by an anti-Dig monoclonal antibody labeled with HRP. **B)** The beads are magnetically attracted to the surface of a SPAuE. **C)** Differential electrochemical detection of the viral target using the chronoamperometry technique.

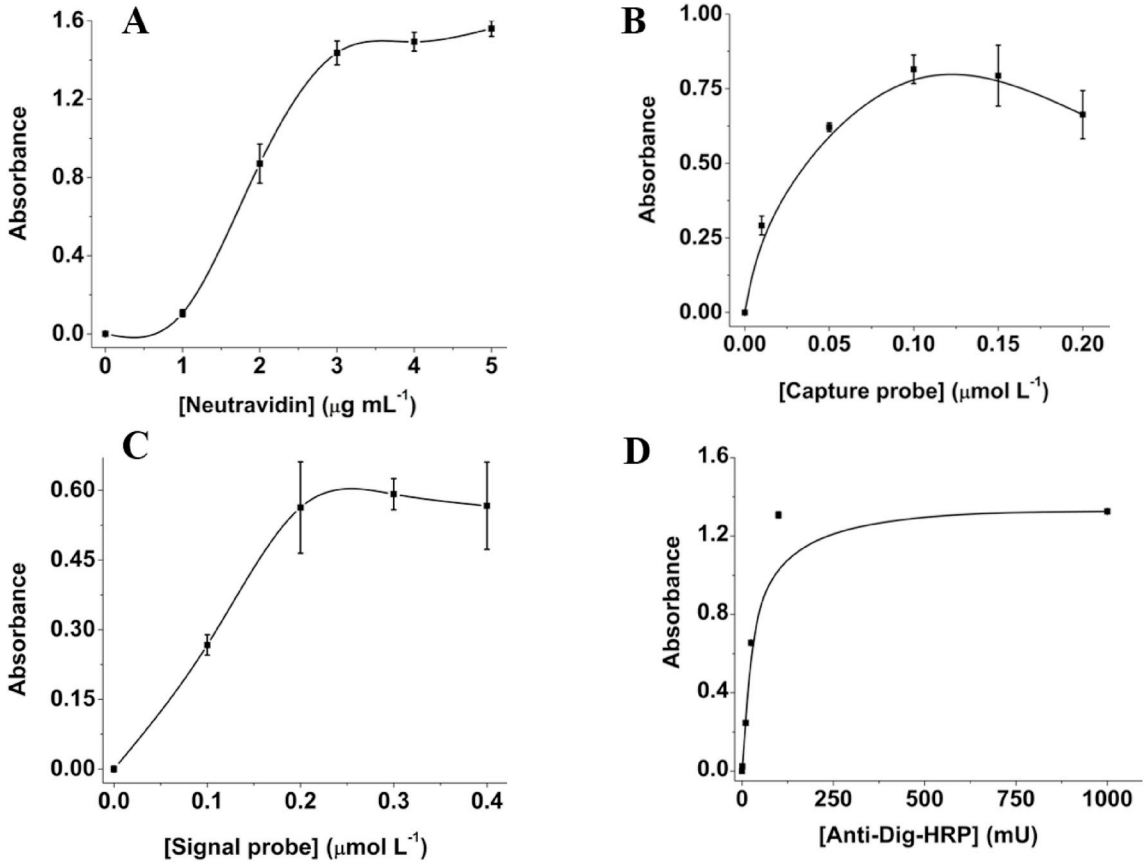

Fig. 2. Optimization of the genosensor assembly. A) neutravidin, **B)** capture probe, **C)** signal probe and **D)** anti-Dig-HRP concentrations optimized by spectrophotometric measurements. All trials correspond to triplicate tests and bars indicate the standard deviation among them. The genosensor was assembled with synthetic capture, signal and target probes of R1 (see Table 1), all other experimental details are in materials and methods and S.I. sections.

Higher protein concentration didn't show any signal improvement (Fig. 2A), whereby 3 μgmL^{-1} of neutravidin was defined as the optimal concentration and fixed-parameter for subsequent experiments. The protein served as an anchor point of the capture probe, whose concentration was varied from 10 nmol L^{-1} to 1 μmol L^{-1}. The colorimetric signal reaches a maximum response at 0.1 μmol L^{-1} capture probe (Fig. 2B), where anchoring capacity of the capture probe by supramolecular junctions with the neutravidin-coated surface is maximum. 0.1 μmol L^{-1} was then the optimal concentration of the capture probe selected. Higher concentrations impact negatively on the signal intensity and on the standard deviation of the measurements because hybridization might be significantly hampered by the steric effect within a dense monolayer of DNA capture probes [28–30]. The concentration of the signal probe was tested from 10 nmol L^{-1} to 0.4 μmol L^{-1}, with 0.2 μmol L^{-1} the concentration that generated the highest colorimetric signal. Higher values generated slightly lower current intensities and higher variability (Fig. 2C). The anti-Dig-HRP antibody was finally interrogated in a concentration ranging from 10 to 1000 mU, with an optimal concentration of 75 mU in the colorimetric format. A higher concentration of anti-Dig-HRP didn't increase the signal, indicating the saturation point (Fig. 2D). The variability of signals was studied by triplicate in each of the tests in all the optimization trials and the optimal conditions were selected by taking into account the signal/noise ratio, *i.e.* the ratio between the signal in the presence and in the absence of target. Other variables were optimized, including temperature and hybridization time, as well as agitation conditions, ionic strength; and time and number of washing steps (results not shown).

One of the most critical steps in obtaining reproducibility and repeatability among experiments is the capture probe incubation conditions, as the basis for the entire assembly. As is known, ions stabilize the phosphate backbone of the DNA chain of the probes by electrostatic repulsion forces, increasing its stability [31]. To evaluate the optimal ionic strength to anchoring the capture probe, it was dissolved in aqueous solutions of different ionic strength by increasing the concentration of NaCl. The optimum NaCl concentration was 0.1 M, as shown in the S.I Fig. S3. Table 2 summarizes the parameters optimized in the genosensor assembly.

Once all variables involved in the biosensor assembly were optimized, we built calibration curves by plotting the resultant colorimetric signal while the concentration of synthetic target DNA was increased. Optimal hybridization time and temperature found by PCR assays for each set of probes in all protocols of sensor development were maintained for all optimization experiments, as detailed in Table 2. During the hybridization step, the biotinylated probes anchored at the surface of neutravidin-sensitized wells come into contact with the conserved

Table 2
Parameters optimized in the genosensors assembly.

Optimized parameter	Range studied	Optimal Condition
Hybridization Temperature	48–62 °C	R1 = 55 °C R2 = 50 °C R5.1-R5.2 = 60 °C
[Neutravidin]	1-10 μgmL^{-1}	3 μgmL^{-1}
[Capture Probe]	0.01–0.5 μmol L^{-1}	0.1 μmol L^{-1}
[Signal Probe]	0.01–0.5 μmol L^{-1}	0.2 μmol L^{-1}
[anti-Dig-HRP] Colorimetric	1–1000 mU	75 mU
[anti-Dig-HRP] Electrochemical	1–1000 mU	200 mU
[NaCl]	0.1–2 M	0.1 M

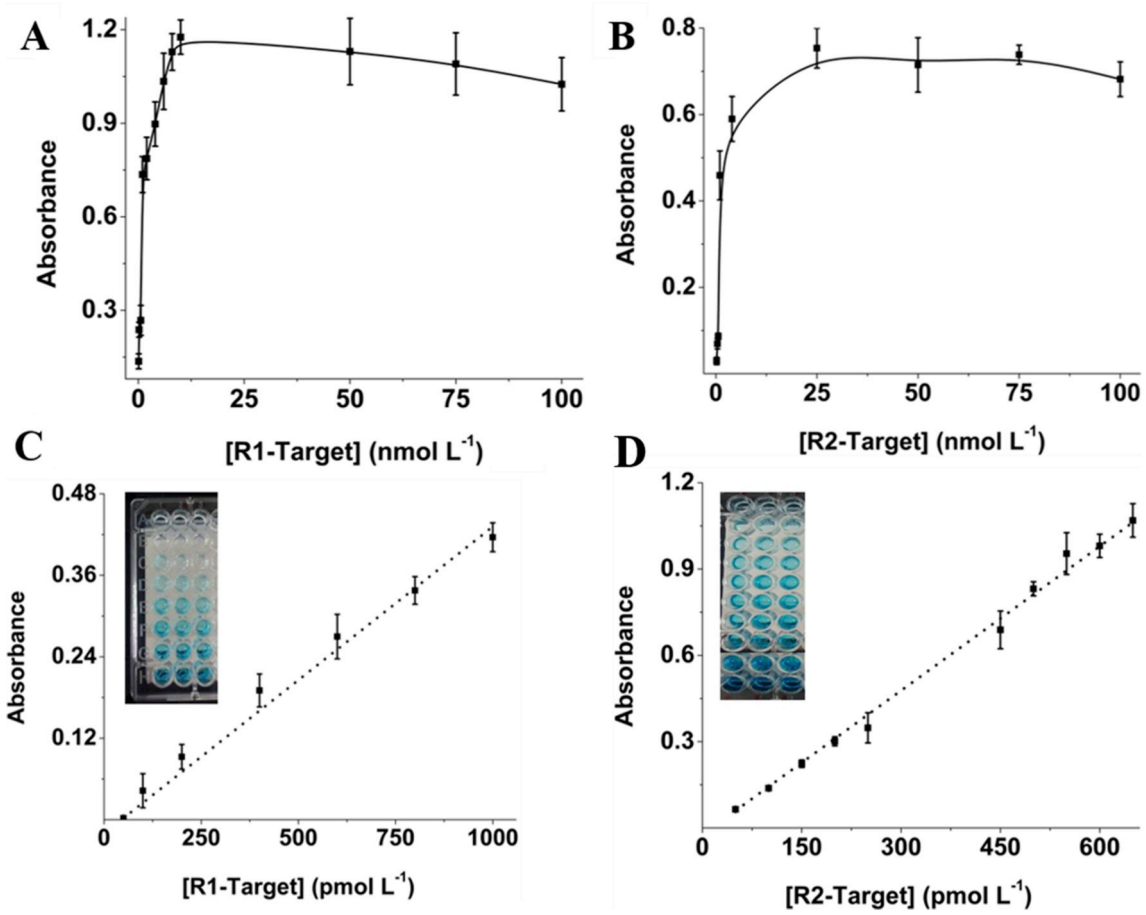

Fig. 3. The colorimetric response of the assembled genosensors. Absorbance profile as the concentration of the conserved regions of the ZIKV synthetic target went from 0.1 to 100 nmol L^{-1} for R1 (A) and R2 (B), respectively. Corresponding calibration curves (C and D) in the linear response regions and raw colorimetric response (in the inset), respectively. Error bars indicate the standard deviation of 3 measurements. The genosensors were assembled with synthetic capture, signal and target probes of R1 and R2 (see Table 1), all other experimental details are in materials and methods and S.I. sections.

Table 3
Analytical performance of the genosensors in both the colorimetric and the electrochemical formats for the regions 1 and 2.

Colorimetric format				
Region	**Linear range (nmol L^{-1})**	**Sensitivity (L $pmol^{-1}$)**	**LOD (pmol L^{-1})**	**R^2 (n = 12)**
R1	0.1–10	0.426	32	0.9934
R2	0.5–7	1.630	9	0.9975
Electrochemical format				
Region	**Linear range (pmol L^{-1})**	**Sensitivity (μA L $pmol^{-1}$)**	**LOD (pmol L^{-1})**	**R^2 (n = 5)**
R1	5–300	0.155	0.7	0.9813
R2	5–400	0.071	3	0.9956

genetic sequences and the signal probes. The complementarity of the DNA strands as well as the optimum incubation time, temperature and agitation favor the interactions in the coupling process from the thermodynamic and kinetic point of view, which ends in the formation of a DNA helix or double-stranded structure. The establishment of the double helix allows a supramolecular arrangement in which the gene sequence to be detected is in the middle of the capture and signal probes in a sandwich-type recognition format, as mentioned. Experiments for all sensors assembled on different days are repeatable with low standard deviations in the linear response regions. Standard deviations increased after reaching the saturation point in each system. Fig. 3 shows the absorbance profile with increasing concentrations of the R1 (A) and R2 (B) conserved regions of the ZIKV synthetic target and the corresponding calibration curves (C and D) in the linear response regions, respectively. R5.1 and R5.1 are in S.I Fig. S3. The analytical parameters form all regions, including linear range, sensitivity, LOD and regression coefficient are summarized in Table 3.

Towards the development of a portable diagnosis tool that can be implemented closer to the patient, we translated the optimized conditions from the genosensor assembled in the microplate format to an electrochemical format. For this purpose, the genosensor was assembled on top of the surface of some paramagnetic sub-micrometer particles that were confined at the surface of a SPAuE. In the presence of H_2O_2, the enzymatically oxidized TMB was reduced back at the surface of the electrode by applying a fixed potential, and the resultant current was recorded for 60 s. To keep homology in the capture probe-functionalized area, we estimated the proper number of magnetic beads whose area correlates well with the area of each microplate, based on the size and concentration of the beads reported by the manufacturer. As 2.57 μl of magnetic beads is equivalent to the area of a functionalized microplate well, we used 3.0 μl of beads for further experiments. We double-checked each variable involved in the electrochemical genosensor assembly by changing one parameter at a time. All results correlated well with those from the colorimetric assay except for the concentration of anti-Dig-HRP, which was optimized again. The concentration of anti-Dig-HRP that generated the higher electrochemical signal with the lower signal/noise ratio was 200 mU (S.I. Fig. 4) so that

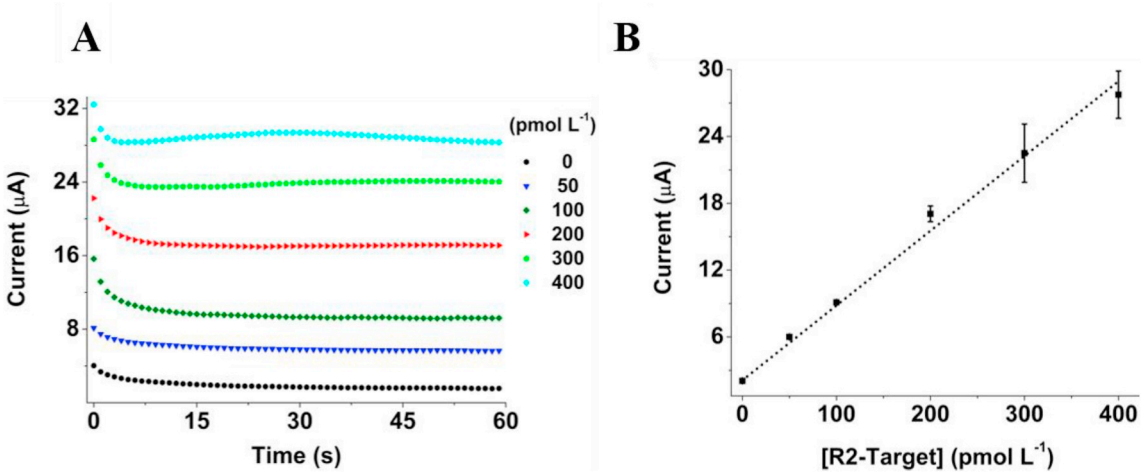

Fig. 4. A) A typical display of target detection by chronoamperometry. Increasing concentrations (0, 50, 100, 200, 300, 400 pmol L^{-1}) of the target R2. **B)** Linear response region for the R1 and R2 genosensors, respectively. The reported currents correspond to the absolute values for the reduction potentials by triplicate. The genosensor was assembled with synthetic capture, signal and target probes of R2 (see Table 1), all other experimental details are in materials and methods and S.I. sections.

this concentration was used for the following experiments. Fig. 4 shows a typical display of the target detection by chronoamperometry, in a current intensity-R2 target concentration-dependent manner (A) and the corresponding calibration curve for R2 (B). The analytical parameters form all regions, are summarized in Table 3. At this point, we demonstrated the differential detection of ZIKV by testing (by triplicate) a dual assay in only one shot with synthetic ZIKV target and RNAase free water as a positive and negative control, respectively, as shown in S.I Fig. 5.

3.3. Detection of genetic material in physiological samples

One of the most challenging issues for applying biosensors in a real scenario is the matrix effect. It is well known that physiological samples are very complex. The coexistence of electrolytes with glucose, lipoproteins, and glycoproteins, lipids, cholesterol, fatty acids, antibodies, among many other molecules may interfere with the biosensor response [32,33]. Interferences may be explained by non-specific interactions between the bioreceptors and the biomolecules (or among the biomolecules) in the matrix; and by the fouling of the electrode, among others. They may be involved in hindering the recognition event or in a poor electron-transfer, thereby impacting on the sensitivity and selectivity of the resultant biosensors [33]. To evaluate the effect that complex matrixes, such as saliva, serum and urine can have in the genosensors response, we challenged the genosensor R1 with physiological samples extracted from a healthy individual spiked with 0.5 nmol L^{-1} of the ZIKV synthetic sequences and compared with samples spiked with the same concentration of DENV and CHIKV genetic material, as explained in the experimental section. The chronoamperometric signals of the genosensor in ZIKV spiked urine, saliva and serum samples were distinguishable from the samples without spiking, which were of the same order of magnitude as a negative control with nuclease-free instead of the complex matrix (see Fig. 5A). It is important to remark that the detection is direct and no PCR amplification is required. These results demonstrated that potential interferences from the complex matrixes do not increase the background signal. Yet, the intensity of the electrochemical signal depends on the physiological sample. For example, the current signals for the spiked urine samples were higher than those from the serum and saliva samples. This result has to do with the high amount of electrolytes found in urine (salts and ionic molecules) that favors the interaction between the DNA strands by diminishing the repulsion forces among them. In contrast, the lowest signal intensity from the saliva sample might be because of the high viscosity of this sample coming from the high concentration of proteins that generates higher resistance to the electron-transfer. The chronoamperometric signals of the genosensors in spiked urine, saliva, and serum samples were consistent with the concentration differences and distinguishable from the samples without spiking, whose signals were of the same order of magnitude as a negative control with nuclease-free water. Then, we compared the response of the genosensor with 0.5 nmol L^{-1} ZIKV sequences with 500 nmol L^{-1} of the arbovirus counterparts in the urine sample. In spite of the concentration of DENV and CHIKV genetic material in the sample was in a 1000-fold excess with respect to the ZIKV, the signal from the ZIK-spiked sample was much higher. Detection of ZIKV in urine is relevant considering that after the end of the viremia stage, the viral loads occurring in the subsequent period (the viruria) are expected to be much higher, thus the detection in urine would be easier. We also compared the response of the genosensor to the ZIKV *versus* those from multiple molecular targets by having either two different DENV sequences or two different CHIKV sequences in a urine sample, with all the tested sequences at an equimolar concentration of 500 pmol L^{-1} (Fig. 5C). The signal for the ZIKV was again much higher with respect to the others, in which the signal was in the order of magnitude as a negative control with non-target. These results demonstrated the potential of the approach for specific detection of the ZIKV in a complex matrix.

We further tested the potential of the genosensors for the detection of the ZIKV in conditions closer to diagnosis in a real scenario. We tested the responses not only in the urine matrix spiked with viral RNA extracted from an infected patient but also in the matrix spiked with cDNA samples from three patients infected with the virus after reverse RNA transcription and RNA from a patient infected with ZIKV (after denaturation). Afterward, we compared the results with respect to those from a synthetic molecular target at a final concentration of 10 pmol L^{-1} as a positive control and nuclease-free water as a negative control.

The resultant chronoamperometric signals exhibited a differential response with significant statistical differences when analyzed by a paired *t*-test and a 1-way ANOVA with a level of statistical significance of 95% (Fig. 5D). Although this test is only a first approximation to a real situation, the different trend of the genosensors response was evident. Although the device requires validation to be used as an analytical tool for diagnostic of ZIKV, this is a proof-of-concept that shows the potential of these devices for differential diagnosis of ZIKV and its discrimination against homologous viruses, such as DENV and CHIKV.

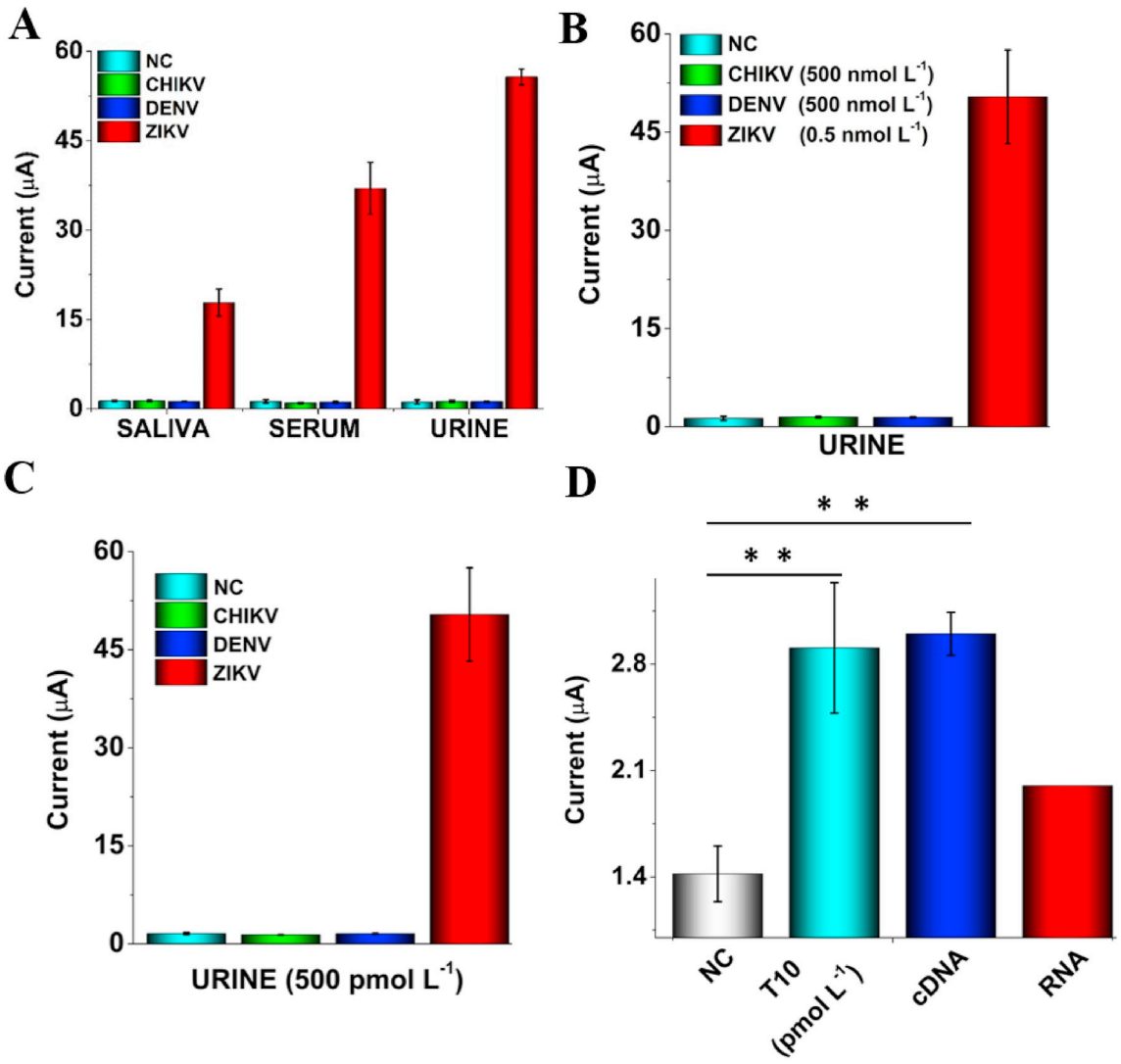

Fig. 5. The electrochemical response of R1 assembled genosensor. A) Genosensors in saliva, serum and urine for ZIKV, DENV, and CHIKV physiological samples at 500 nmol L^{-1}. B) Molecular targets of DENV and CHIKV in a 1000-fold excess with respect to the ZIKV concentration. C) Multiple molecular targets of DENV and CHIKV (two different strands each) with respect to the ZIKV target stand. Negative controls contain all components of the genosensor including the biological matrix except for the viral synthetic target. D) The response of the genosensors to samples of infected patients. cDNA from three infected patients and RNA from one ZIKV infected patient, synthetic molecular target at a final concentration of 10 pM (T-10 pmol L^{-1}) and RNase-free water as the positive and negative control (NC), respectively. **Indicate significant statistical differences ($P < 0.01$).

4. Conclusion

We presented the development of genosensors for the differential detection of the ZIKV and its discrimination against homologous arboviruses, such as DENV and CHIKV. From a robust and rigorous bioinformatic analysis, we designed four conserved regions for the specific detection of the ZIKV, the forward and reverse primers for the target amplification, and a 3′-end biotinylated capture probe and a 5′ end Dig-labeled signal probe for assembling the genosensor, per each of the four selected targets. Specificity was probed by conventional and real-time PCR tests, thus ensuring the subsequent development of the PCR amplification-free and differential genosensors. We optimized the hybridization conditions in a colorimetric and an electrochemical format, offering opportunities for bench and portable detection of the virus. We studied the analytical performance of the genosensors in buffered and spiked solutions with synthetic DNA from the ZIKV and built calibration curves in both formats. To move towards the differential detection of the ZIKV, we evaluated the effect of saliva, serum and urine sample matrixes on the resultant analytical signal and demonstrated the potential for differential detection against the synthetic genetic material of DENV and CHIKV. We tested the responses in the urine matrix not only spiked with viral RNA extracted from an infected patient but also with cDNA samples from three patients infected with the virus after reverse RNA transcription; and RNA from a ZIKV infected patient after denaturation. Current work is directed to decrease the LOD of the genosensor down to the fM range, to achieve the detection of clinically relevant concentrations of ZIKV and validate the diagnosis tool in real samples. Overall, the bio-platforms proved to be promising for the development of easy-to-use portable devices for virus diagnosis closed to the patient.

Declaration of competing interest

The authors declare there is no conflict of interest.

Acknowledgements

The work has been funded by COLCIENCIAS, through the 111574454836 project. J.O thanks support from The University of Antioquia and The Max Planck Society through the cooperation

agreement 566–1, 2014. Authors thank Mr. Esteban Marín from the PECET (Universidad de Antioquia) for his technical support in the molecular methods. We acknowledge to Dr. Raquel E. Ocazionez from The Medical School, Centro de Investigaciones en Enfermedades Tropicales (Universidad Industrial de Santander) and Dr. Salim Mattar, Instituto de Investigaciones Biológicas del Trópico IIBT (Universidad de Cordoba) for providing us with virus isolates and serum samples from infected patients, respectively.

Appendix A. Supplementary data

Supplementary data to this article can be found online at https://doi.org/10.1016/j.talanta.2019.120648.

References

[1] A. Gulland, Zika virus is a global public health emergency, declares WHO, Bmj 657 (2016) i657, https://doi.org/10.1136/bmj.i657.
[2] E. Camacho, M. Paternina-Gomez, P.J. Blanco, J.E. Osorio, M.T. Aliota, Detection of autochthonous zika virus transmission in Sincelejo, Colombia, Emerg. Infect. Dis. 22 (2016) 927–929, https://doi.org/10.3201/eid2205.160023.
[3] D. Musso, C. Roche, T.X. Nhan, E. Robin, A. Teissier, V.M. Cao-Lormeau, Detection of Zika virus in saliva, J. Clin. Virol. 68 (2015) 53–55, https://doi.org/10.1016/j.jcv.2015.04.021.
[4] G. Kuno, Universal diagnostic RT-PCR protocol for arboviruses, J. Virol. Methods 72 (1998) 27–41, https://doi.org/10.1016/S0166-0934(98)00003-2.
[5] M.P. Fernandez, E.P. Saad, M.O. Martinez, S. Corchuelo, M.M. Reyes, M.J. Herrera, M.P. Saavedra, A. Rico, A.M. Fernandez, R.K. Lee, C.V. Ventura, A.M. Berrocal, S.R. Dubovy, Ocular Histopathologic Features of Congenital Zika Syndrome, (2017), pp. 1–7, https://doi.org/10.1001/jamaophthalmol.2017.3595.
[6] V.-M. Cao-Lormeau, A. Blake, S. Mons, S. Lastère, C. Roche, J. Vanhomwegen, T. Dub, L. Baudouin, A. Teissier, P. Larre, A.-L. Vial, C. Decam, V. Choumet, S.K. Halstead, H.J. Willison, L. Musset, J.-C. Manuguerra, P. Despres, E. Fournier, H.-P. Mallet, D. Musso, A. Fontanet, J. Neil, F. Ghawché, Guillain-Barré Syndrome outbreak associated with Zika virus infection in French Polynesia: a case-control study, Lancet 387 (2016) 1531–1539, https://doi.org/10.1016/S0140-6736(16)00562-6.
[7] R. da Fonseca Alves, D.L. Franco, M.T. Cordeiro, E.M. de Oliveira, R.A. Fireman Dutra, M. Del, Pilar Taboada Sotomayor, Novel electrochemical genosensor for Zika virus based on a poly-(3-amino-4-hydroxybenzoic acid)-modified pencil carbon graphite electrode, Sens. Actuators B Chem. 296 (2019) 126681, , https://doi.org/10.1016/j.snb.2019.126681.
[8] H.A.M. Faria, V. Zucolotto, Label-free electrochemical DNA biosensor for zika virus identification, Biosens. Bioelectron. 131 (2019) 149–155, https://doi.org/10.1016/j.bios.2019.02.018.
[9] G. Cabral-Miranda, A.R. Cardoso, L.C.S. Ferreira, M.G.F. Sales, M.F. Bachmann, Biosensor-based selective detection of Zika virus specific antibodies in infected individuals, Biosens. Bioelectron. 113 (2018) 101–107, https://doi.org/10.1016/j.bios.2018.04.058.
[10] K. Takemura, O. Adegoke, T. Suzuki, E.Y. Park, A localized surface plasmon resonance-amplified immunofluorescence biosensor for ultrasensitive and rapid detection of nonstructural protein 1 of Zika virus, PLoS One 14 (2019) 1–14, https://doi.org/10.1371/journal.pone.0211517.
[11] O. Adegoke, M. Morita, T. Kato, M. Ito, T. Suzuki, E.Y. Park, Localized surface plasmon resonance-mediated fluorescence signals in plasmonic nanoparticle-quantum dot hybrids for ultrasensitive Zika virus RNA detection via hairpin hybridization assays, Biosens. Bioelectron. 94 (2017) 513–522, https://doi.org/10.1016/j.bios.2017.03.046.
[12] W. Sukjee, T. Jaimipuk, A. Thitithanyanont, C. Sangma, C. Thepparit, P. Auewarakul, C. Tancharoen, Electrochemical biosensor based on surface imprinting for Zika virus detection in serum, ACS Sens. 4 (2018) 69–75, https://doi.org/10.1021/acssensors.8b00885.
[13] R. Wu, Y. Ma, J. Pan, S.H. Lee, J. Liu, H. Zhu, R. Gu, K.J. Shea, G. Pan, Efficient capture, rapid killing and ultrasensitive detection of bacteria by a nano-decorated multi-functional electrode sensor, Biosens. Bioelectron. 101 (2018) 52–59, https://doi.org/10.1016/j.bios.2017.10.003.
[14] B. Koo, C.E. Jin, T.Y. Lee, J.H. Lee, M.K. Park, H. Sung, S.Y. Park, H.J. Lee, S.M. Kim, J.Y. Kim, S.H. Kim, Y. Shin, An isothermal, label-free, and rapid one-step RNA amplification/detection assay for diagnosis of respiratory viral infections, Biosens. Bioelectron. 90 (2017) 187–194, https://doi.org/10.1016/j.bios.2016.11.051.
[15] L. Wang, J.E. Filer, M.M. Lorenz, C.S. Henry, D.S. Dandy, B.J. Geiss, An ultra-sensitive capacitive microwire sensor for pathogen-specific serum antibody responses, Biosens. Bioelectron. 131 (2019) 46–52, https://doi.org/10.1016/j.bios.2019.01.040.
[16] D. Han, R. Chand, Y.S. Kim, Microscale loop-mediated isothermal amplification of viral DNA with real-time monitoring on solution-gated graphene FET microchip, Biosens. Bioelectron. 93 (2017) 220–225, https://doi.org/10.1016/j.bios.2016.08.115.
[17] J. Orozco, L.K. Medlin, Electrochemical performance of a DNA-based sensor device for detecting toxic algae, Sens. Actuators B Chem. 153 (2011) 71–77, https://doi.org/10.1016/j.snb.2010.10.016.
[18] J. Orozco, C. Jiménez-Jorquera, C. Fernández-Sánchez, Gold nanoparticle-modified ultramicroelectrode arrays for biosensing: a comparative assessment, Bioelectrochemistry 75 (2009) 176–181, https://doi.org/10.1016/j.bioelechem.2009.03.013.
[19] D. Wang, H. Hua, H. Tang, C. Yang, W. Chen, Y. Li, A signal amplification strategy and sensing application using single gold nanoelectrodes, Analyst 144 (2019) 310–316, https://doi.org/10.1039/c8an01474d.
[20] X. Zhao, R. Tapec-Dytioco, W. Tan, Ultrasensitive DNA detection using highly fluorescent bioconjugated nanoparticles, J. Am. 125 (2003) 11474–11475 http://pubs.acs.org/doi/abs/10.1021/ja0358854.
[21] J. Orozco, J. Baudart, L.K. Medlin, Evaluation of probe orientation and effect of the digoxigenin-enzymatic label in a sandwich hybridization format to develop toxic algae biosensors, Harmful Algae 10 (2011) 489–494, https://doi.org/10.1016/j.hal.2011.03.004.
[22] J. Orozco, L.K. Medlin, Electrochemical performance of a DNA-based sensor device for detecting toxic algae, Sens. Actuators B Chem. 153 (2011) 71–77, https://doi.org/10.1016/j.snb.2010.10.016.
[23] C.L.B. Gadia, A. Manirakiza, G. Tekpa, X. Konamna, U. Vickos, E. Nakoune, Identification of pathogens for differential diagnosis of fever with jaundice in the Central African Republic: a retrospective assessment, 2008-2010, BMC Infect. Dis. 17 (2017) 1–5, https://doi.org/10.1186/s12879-017-2840-8.
[24] P. Krejbich-Trotot, B. Gay, G. Li-Pat-Yuen, J.J. Hoarau, M.C. Jaffar-Bandjee, L. Briant, P. Gasque, M. Denizot, Chikungunya triggers an autophagic process which promotes viral replication, Virol. J. 8 (2011) 1–10, https://doi.org/10.1186/1743-422X-8-432.
[25] D. Warrilow, J.A. Northill, A. Pyke, G.A. Smith, Single rapid TaqMan fluorogenic probe based PRC assay that detects all four dengue serotypes, J. Med. Virol. 66 (2002) 524–528, https://doi.org/10.1002/jmv.2176.
[26] J.E. Fraser, J.T. De Bruyne, I. Iturbe-Ormaetxe, J. Stepnell, R.L. Burns, H.A. Flores, S.L. O'Neill, Novel Wolbachia-transinfected Aedes aegypti mosquitoes possess diverse fitness and vector competence phenotypes, PLoS Pathog. 13 (2017) 1–19, https://doi.org/10.1371/journal.ppat.1006751.
[27] E. Rancès, Y.H. Ye, M. Woolfit, E.A. McGraw, S.L. O'Neill, The relative importance of innate immune priming in Wolbachia-mediated dengue interference, PLoS Pathog. 8 (2012), https://doi.org/10.1371/journal.ppat.1002548.
[28] J. Zhang, S. Song, L. Zhang, L. Wang, H. Wu, D. Pan, C. Fan, Sequence-specific detection of femtomolar DNA via a chronocoulometric DNA sensor (CDS): effects of nanoparticle-mediated amplification and nanoscale control of DNA assembly at electrodes, J. Am. Chem. Soc. 128 (2006) 8575–8580.
[29] K.J. Huang, Y.J. Liu, J.Z. Zhang, J.T. Cao, Y.M. Liu, Aptamer/Au nanoparticles/cobalt sulfide nanosheets biosensor for 17β-estradiol detection using a guanine-rich complementary DNA sequence for signal amplification, Biosens. Bioelectron. 67 (2015) 184–191.
[30] J. Chen, C. Ye, Z. Liu, L. Yang, A. Liu, G. Zhong, H. Peng, X. Lin, Facilely prepared low-density DNA monolayer–based electrochemical biosensor with high detection performance in human serum, Anal. Bioanal. Chem. 411 (2019) 2101–2109.
[31] J. Orozco, E. Villa, C.L. Manes, L.K. Medlin, D. Guillebault, Electrochemical RNA genosensors for toxic algal species: enhancing selectivity and sensitivity, Talanta 161 (2016) 560–566, https://doi.org/10.1016/j.talanta.2016.08.073.
[32] L. Johnsson, G.A. Baxter, S.R.H. Crooks, D.L. Brandon, C.T. Elliott, Reduction of sample matrix effects - the analysis of benzimidazole residues in serum by immunobiosensor, Food Agric. Immunol. 14 (2002) 209–216, https://doi.org/10.1080/09540100220145000a.
[33] J. Sun, Y. Liu, Matrix effect study and immunoassay detection using electrolyte-gated graphene biosensor, Micromachines 9 (2018) 142, https://doi.org/10.3390/mi9040142.